MOLECULAR PHYSICS, 1989, VOL. 66, NO. 2, 493–507

Nematic liquid crystals

A Monte Carlo simulation study in higher dimensions

by MICHAEL E. MANN, CHRISTOPHER H. MARSHALL
and A. D. J. HAYMET
Department of Chemistry, University of California,
Berkeley, California 94720, U.S.A.

(*Received 18 July 1988; accepted 20 September 1988*)

The Lebwohl–Lasher model of the isotropic–nematic phase transition in liquid crystals is studied in higher dimensions, by Monte Carlo computer simulations on simple cubic lattices. The transition is found to become increasingly first-order, and rapidly approaches the mean-field results, which are exact in infinitely many dimensions. The discontinuities in internal energy and order parameter are measured by careful analysis of the computer simulation data, and the free energy of each system is calculated. An empirical scaling law is also found to describe the shift of the transition temperature from the mean-field theory result. To distinguish the effects of coordination number from those of dimension and connectivity, a simulation of an f.c.c. lattice in $d = 3$ dimensions is performed. In addition, a partial analysis is made of finite-size effects in the six-dimensional simulation.

1. Introduction

The isotropic–nematic transition in liquid crystals is a 'weak' first-order phase transition in three dimensions ($d = 3$). Although more faithful models of nematogens exist [1, 2], we study here the Lebwohl–Lasher nearest neighbour spin model of the isotropic–nematic transition [3] because its transition properties show an uncanny resemblance to the actual transition. In two dimensions, this spin model displays a second-order transition. This work studies the transition in higher spatial dimensions.

In any dimension, the transition could be first or second-order (or even something else). If the transition remains first-order, as one expects, it will approach the result of mean-field theory as the dimension, and number of nearest neighbours, grow large. This result follows because in infinitely many dimensions each particle feels the average field due to an infinite number of neighbours. If the phase transition were second-order, according to renormalization group theory, mean-field theory would be correct above some critical dimension d^* (in this case 6) characteristic of the hamiltonian under study [4]. Our simulations in $d = 3$, 4, 5, and 6 confirm that the transition remains first-order, and approaches the mean-field result quite rapidly. The question then remains as to how the properties of a first-order transition approach the mean-field results as the spatial dimension of the system is increased. This is the central question addressed here.

The Maier–Saupe model [5] of the istropic–nematic phase transition for liquid crystals is the appropriate model to investigate, since it is both simple and has a weak first-order transition in three dimensions [3, 6], in marked contrast to mean-

field theory of the same model [5, 7]. We perform Monte Carlo simulations on the simplified Lebwohl–Lasher model, which consists of uniaxial 3-dimensional rod-like molecules (called 'spins' by analogy with the Heisenberg ferromagnet) fixed on a regular lattice in d dimensions and obeying periodic boundary conditions. The spins interact via the potential energy

$$U = -\varepsilon \sum_{\langle i,j \rangle} P_2(\cos \theta_{ij}), \tag{1}$$

where $\langle i, j \rangle$ indicates that the sum is to be taken over all nearest neighbour pairs of spins, θ_{ij} is the angle between neighbouring spin axes, and ε sets the interaction energy scale. This model undergoes a transition from a disordered (isotropic) phase to an ordered (nematic) phase as the temperature is lowered.

We consider simple cubic lattices of dimension $d = 3$, 4, 5, 6, for which the coordination number is $z = 2d$. The computational details of our simulations are summarized in §2. In §3 we study the effect of increasing dimension on the transition behaviour of the Lebwohl–Lasher model, and in particular we compare results obtained for each dimension with the predictions of mean-field theory. To distinguish the effect of dimensionality and connectivity from a simple coordination number effect, we also perform simulations on a $d = 3$ f.c.c. lattice, which has coordination number $z = 12$. Therefore, we can make comparisons with both the $d = 3$ and $z = 12$ ($d = 6$) simple cubic lattice results. Finally, we consider finite-size effects by examining the six-dimensional simple cubic system with linear dimensions $L = 3$, 4, 5. In doing so, we test the validity of using a relatively small linear dimension in higher spatial dimensions to obtain the thermodynamic quantities of interest [8]. Our conclusions are collected in §4.

2. Computational details

In our Monte Carlo simulations, a partially vectorized version of the standard Metropolis sampling algorithm [9] was used. For each system, two initial conditions were used, an ordered configuration for 'heating' runs and a randomly oriented configuration for 'cooling' runs. Quantities tabulated for each temperature include the reduced temperature, $T^* = kT/\varepsilon$, $\beta^* = 1/T^*$, the average internal energy per particle $\langle U^* \rangle = \langle U \rangle / N\varepsilon$, where N is the total number of spins, the average square internal energy per particle $\langle U^{*2} \rangle = \langle U^2 \rangle / (N\varepsilon)^2$, and the long-range order parameter $M = \langle P_2(\cos \theta_i) \rangle$, where θ_i is the angle between the axis of the ith spin and the director. Since the director, which measures the average orientation of the system, usually fluctuates over the course of a simulation, the order parameter has been calculated as the dominant eigenvalue of the orientation tensor

$$Q_{ij} = \tfrac{3}{2}\langle c_i c_j \rangle - \tfrac{1}{2}\delta_{ij}, \tag{2}$$

where c_i and c_j refer to direction cosines of the spin axes, and i and j are taken over x, y, and z directions. The angle brackets indicate an ensemble average [10]. For systems of approximately 4000 spins, about 12 000 cycles through the system were performed for each temperature, with 3000 cycles for equilibration. To ensure comparable statistics for systems of different sizes, appropriately more cycles per temperature were taken for smaller systems. Because the calculation of the order parameter is computationally intensive, it was not performed at every cycle. Instead,

it was found that this calculation could be performed every 5 cycles without loss of vital information.

The heat capacity of the system was calculated both from fluctuations in the internal energy,

$$C_v^* = N\beta^{*2}(\langle U^{*2}\rangle - \langle U^*\rangle^2), \tag{3}$$

and from a numerical, spline derivative of the internal energy, although the former method proved to be more reliable. Approximately 40 steps in reciprocal temperature β^* were taken for each run, with smaller steps taken in the transition region. In addition, approximately twice as many cycles were taken for temperatures very close to the transition. Heating runs were started with all particles aligned along the director axis at a value for β of the order of $\beta^* = 10$ while cooling runs were started with an initially random configuration and a value of approximately $\beta^* = 0{\cdot}01$. Starting configurations for subsequent temperatures were borrowed from the final configuration for the previous temperature.

Spin configurations were stored as three direction cosines for each particle, and new values were generated randomly over the unit sphere to ensure proper sampling of phase space. Reasonable acceptance ratios were obtained for all temperatures of interest. All simulations were performed on a Cray XMP-14 using a partially vectorized code. The Cray RANF routine was used to generate random numbers. For systems of about 4000 spins, both cooling and heating runs (at 80 temperatures) consumed approximately 9 hours of CPU time. Due to certain vector loops, run time was approximately linear in the number of spins.

To facilitate comparison of results between different dimensions, we have adopted the following conventions. The energy (and hence the inverse temperature β, since it is only the product of that two that enters into the calculations) scale with the coordination number z and hence with d. Consequently, we have normalized the energy and inverse temperature β to the familiar three-dimensional (or more precisely, $z = 6$) convention, used for example by Luckhurst and collaborators [10]. For example, in six dimensions ($z = 12$) the inverse temperature at the transition, β_c^*, has been multiplied by 2, and the jump in internal energy at the transition ΔU_c has been divided by 2.

3. Results and discussion

3.1. *Simple cubic lattice in many dimensions*

Simulations were performed on systems of 16^3, 8^4, 5^5, and 4^6 spins in an attempt to keep the system size close to 4000 spins for all dimensions. In figure 1 we display, for each dimension, the internal energy U^* as a function of temperature *and* inverse temperature β^* on a large scale. The order parameter M is shown on this same scale in figure 2. Precise values of the transition temperature $T_c^* = 1/\beta_c^*$ were determined from the locations of the maxima in the heat capacities, shown in figure 3. As explained below, when hysteresis was observed from comparison of cooling and heating runs, the heating run gave the more accurate value for the transition temperature. The values of the discontinuity in the internal energy ΔU_c were obtained by extrapolation of the points corresponding to the nematic ($T^* < T_c^*$) and isotropic ($T^* > T_c^*$) phases to the determined transition temperature. These extrapolations were assisted by using two independent smoothing spline fits, and are shown

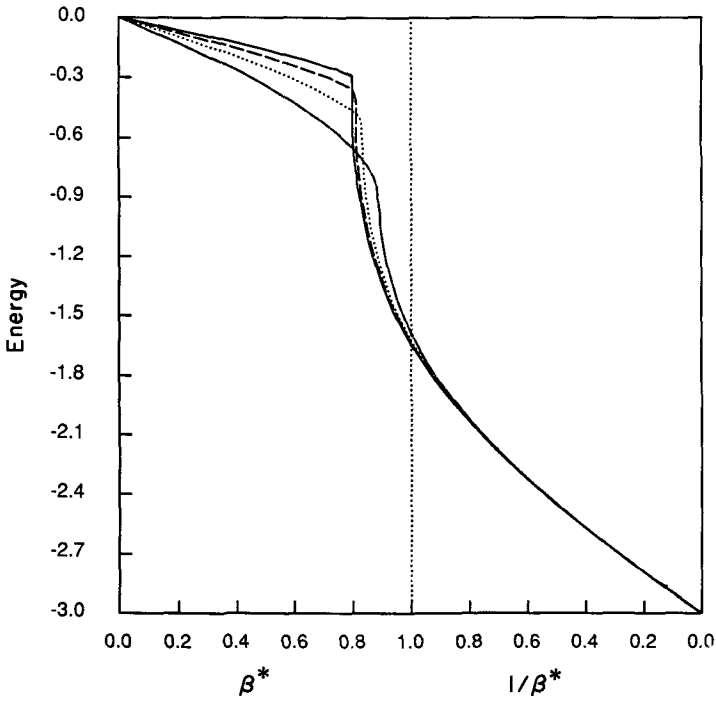

Figure 1. The internal energy U^* as a function of the temperature $1/\beta^*$ and β^* for simple cubic lattices of dimension 6 (solid line), 5 (dashed), 4 (dotted) and 3 (dot–dashed), on a large scale.

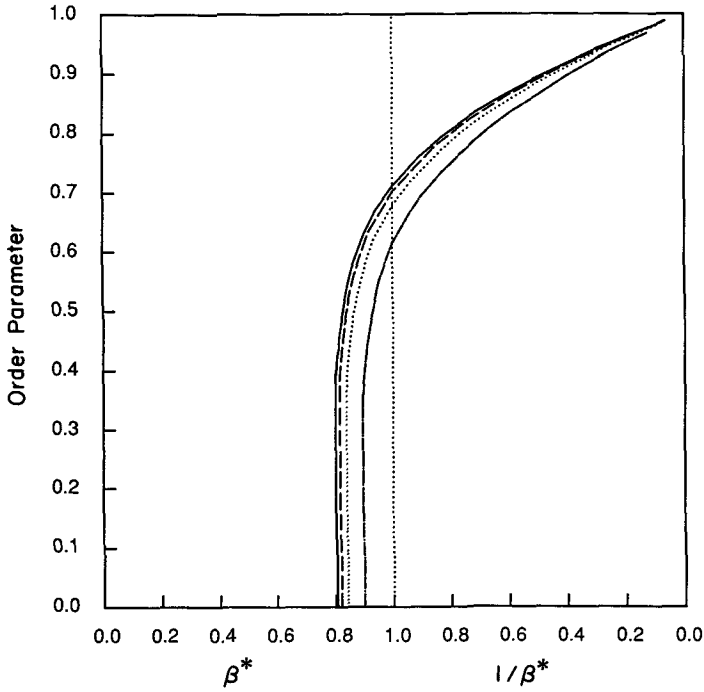

Figure 2. The order parameter M as a function of the temperature $1/\beta^*$ and β^* for simple cubic lattices of dimension 6 (solid line), 5 (dashed), 4 (dotted) and 3 (dot–dashed), on a large scale.

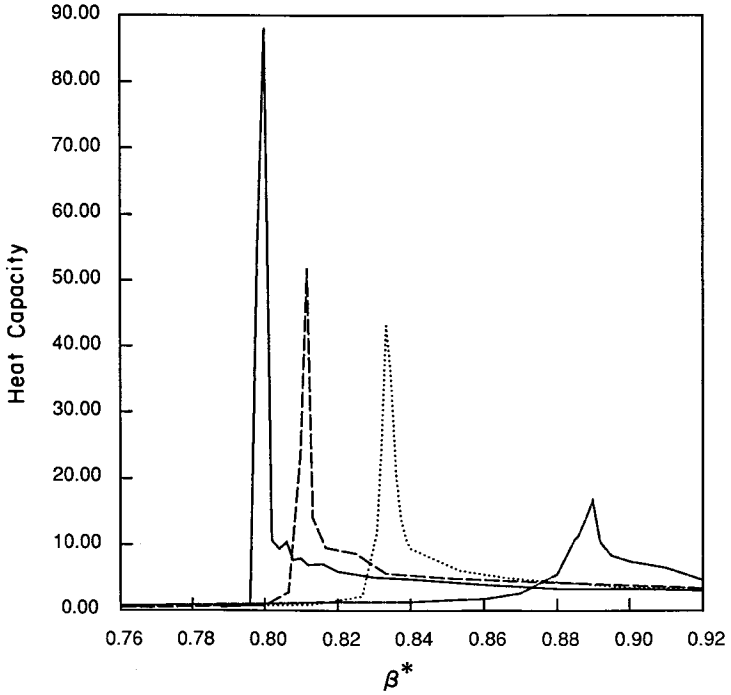

Figure 3. The heat capacity C_v^* as a function of inverse temperature β^* for simple cubic lattices of dimension 6 (solid line), 5 (dashed), 4 (dotted) and 3 (dot–dashed).

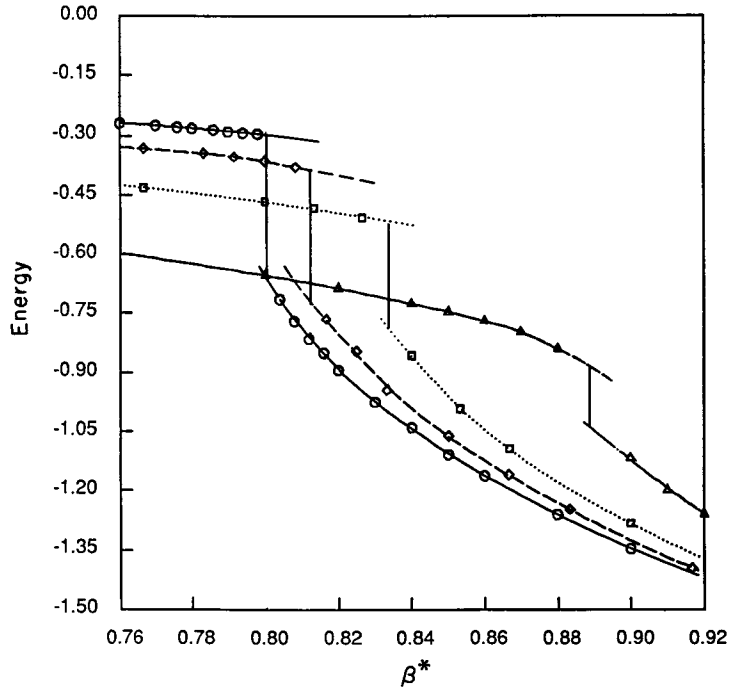

Figure 4. The internal energy U^* as a function of the inverse temperature β^* for simple cubic lattices of dimension 6 (solid line), 5 (dashed), 4 (dotted) and 3 (dot–dashed), near β_c^*, with extrapolations corresponding to the isotropic and nematic phases.

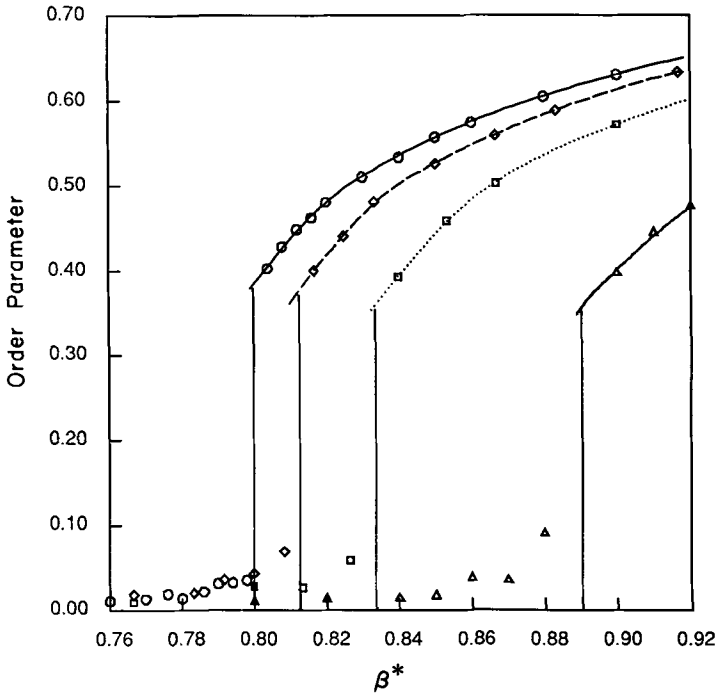

Figure 5. The order parameter M as a function of the temperature β^* for simple cubic lattices of dimension 6 (solid line), 5 (dashed), 4 (dotted) and 3 (dot–dashed), near β_c^*, with extrapolations corresponding to the isotropic and nematic phases.

on a fine scale in figure 4, together with the actual simulation values in the nematic and isotropic phases. Similarly, the values of the order parameter discontinuity at the transition M_c were found by extrapolating the results of the nematic phase to the transition. These extrapolations were also made with the assistance of a smoothing spline fit, and are shown in figure 5 along with the actual simulation results in both the nematic and isotropic phases.

The transition values T_c^*, β_c^*, M_c, and the transition energy ΔU_c as a function of dimension d are collected in table 1, together with the results from mean-field theory. The uncertainties in the location of the transition and in the extrapolations are also indicated. Following the work of Lebwohl and Lasher [3], we calculated

Table 1. Transition properties for simple cubic lattices.

d	β_c^*	M_c	ΔU_c	T_c^*
3	0·890 ± 0·002	0·350 ± 0·020	0·130 ± 0·020	1·124 ± 0·003
4	0·834 ± 0·001	0·370 ± 0·010	0·270 ± 0·010	1·199 ± 0·002
5	0·812 ± 0·002	0·380 ± 0·005	0·320 ± 0·010	1·232 ± 0·003
6	0·800 ± 0·002	0·390 ± 0·005	0·360 ± 0·005	1·250 ± 0·003
MF	0·757	0·429	0·551	1·321

the *free* energy of the system from the formulae

$$\beta f(\beta) = (\beta f)_{\text{high}} - \int_{\beta_{\text{high}}}^{\beta} d\beta \langle U \rangle, \tag{4}$$

$$\beta f(\beta) = (\beta f)_{\text{low}} + \int_{\beta_{\text{low}}}^{\beta} d\beta \langle U \rangle, \tag{5}$$

coupled with both analytically evaluated low and high β limits of the free energy (see Appendix) and the simulation values of $\langle U \rangle$. For a check on the location of the phase transition, one can determine β_c^* from the value of β^* at which a 'kink' in the free energy occurs, and the discontinuity in the energy of transition, ΔU_c, from the slope of f at this point. However, this method involves taking the difference of two large numbers, and in practice, leads to results inferior to those obtained above. The free energies of the systems are plotted in figure 6.

As the dimension increases, the transition becomes increasingly first-order in character. As shown in figure 3, even for finite-sized samples the heat capacity displays a more pronounced divergence for higher dimensions, and, as shown in figure 4, the discontinuity in the energy becomes larger with increasing dimension. This is also demonstrated by the more pronounced kink in the free energies of figure 6 in higher dimensions. In addition, the order parameter drops more abruptly to zero in the isotropic phase in higher dimensions (figure 5), also indicative of increasingly first-order behaviour. There is a rapid approach to the predictions of mean-field theory as the dimension is increased, as shown in table 2.

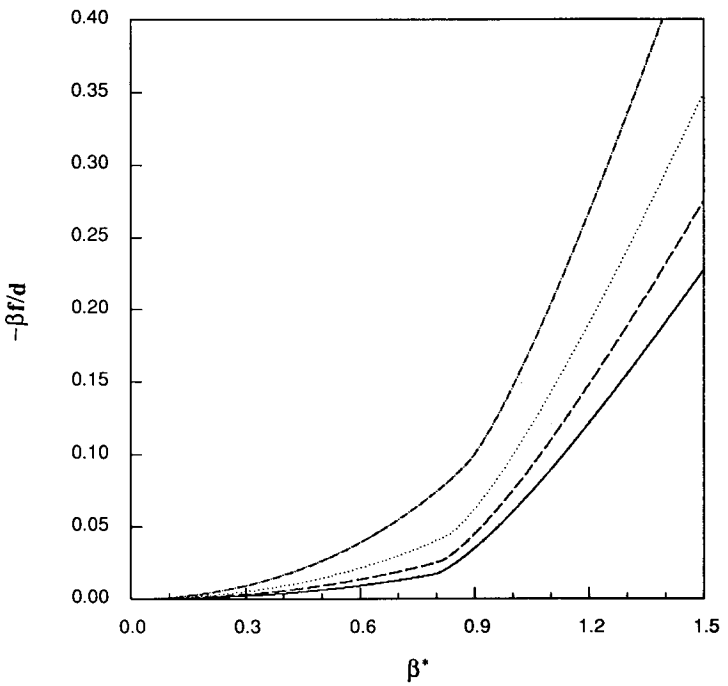

Figure 6. The free energy $-\beta f^*$ as a function of inverse temperature β^*, as calculated in the Appendix, for simple cubic lattices of dimension 6 (solid line), 5 (dashed), 4 (dotted) and 3 (dot–dashed).

Table 2. Comparison with mean-field theory.

d	$\frac{\beta_c^* - \beta_{cMF}^*}{\beta_{cMF}^*}$	$\frac{M_{cMF} - M_c}{M_{cMF}}$	$\frac{\Delta U_{cMF} - \Delta U_c}{\Delta U_{cMF}}$	$\frac{T_{cMF}^* - T_c^*}{T_{cMF}^*}$
3	0·176	0·184	0·764	0·149
4	0·102	0·149	0·510	0·092
5	0·073	0·114	0·419	0·067
6	0·057	0·091	0·347	0·057

To analyse the shift in transition temperature with dimension, we have simply *assumed* that the deviation from the mean-field result follows a power law, similar to that for finite-size scaling of a second-order transition temperature in a fixed dimension. Specifically, we assume

$$T_c^*(d = \infty) - T_c^*(d) \propto d^{-\mu} \tag{6}$$

for some exponent μ, where by the previous argument we can associate $T_c^*(d = \infty)$ with the mean-field result $T_c^* = 1.321$. Of course, such a scaling law could only hold for a first-order transition since it presupposes that a finite upper critical dimension does not exist. Empirically, the result is quite surprising. In figure 7 we display the quantity $W = -\ln (T_c^*(d = \infty) - T_c^*(d))$ as a function of $\ln d$, which should give a line of slope μ. From our limited data, it appears that the presumed power law scaling holds, with an exponent very close to $\mu = 1{\cdot}5$. Although the points corre-

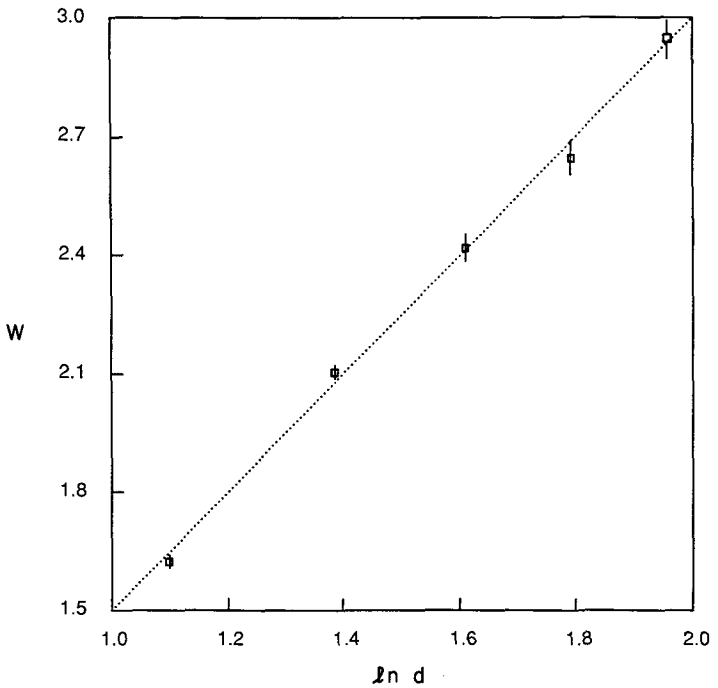

Figure 7. The quantity $W = -\ln (T_c^*(d = \infty) - T_c^*(d))$, defined in the text, as a function of the logarithm of the spatial dimension $\ln d$. The straight line (dotted) has slope $\mu = 1{\cdot}5$.

Table 3. Transition properties for f.c.c. $d = 3$ and simple cubic lattices.

Lattice	β_c^*	M_c	ΔU_c	T_c^*
SC $d = 3$	0·890 ± 0·002	0·350 ± 0·020	0·130 ± 0·020	1·124 ± 0·003
SC $d = 4$	0·834 ± 0·001	0·370 ± 0·010	0·270 ± 0·010	1·199 ± 0·002
SC $d = 6$	0·800 ± 0·002	0·390 ± 0·005	0·360 ± 0·005	1·250 ± 0·003
f.c.c. $d = 3$	0·831 ± 0·002	0·350 ± 0·020	0·160 ± 0·020	1·203 ± 0·003

sponding to $d = 3$ and $d = 4$ do not fall on the line within the uncertainties indicated, one would expect the scaling to be exact only in the asymptotic limit $d \to \infty$, and hence points corresponding to lower values of d might stray from the assumed behaviour. A simulation in seven dimensions, limited to the transition region, for a system of 4^7 spins, also yields agreement with the empirical scaling law. The value of the slope μ is apparently equal to the spin dimension divided by two. Since we known of no theoretical arguments for this phenomenon, other than the plausibility of some kind of power-law scaling for the shift in transition temperature from the mean-field result, we offer it only as an empirical result from the simulations.

3.2. *Comparison of f.c.c. $d = 3$ with simple cubic*

To investigate the relative importance of dimension, connectivity, and coordination number in determining the transition behaviour of the model nematogens, we have performed Monte Carlo simulations on a face centred cubic (f.c.c.) lattice of 4×10^3 spins, which has both dimension $d = 3$ and coordination number $z = 12$, and a different connectivity from the simple cubic lattices [11]. In table 3 we display the results for the $d = 3$ f.c.c. system, together with those simple cubic in $d = 3$, 4, 6 for comparison.

We note that the transition properties on the f.c.c. lattice are much more similar to the $d = 3$ and $d = 4$ simple cubic lattices than to the $d = 6$ simple cubic lattice, which has the same coordination number. In addition, figure 8 shows that the behaviour of the energy as a function of inverse temperature β^* is qualitatively much more like that for the $d = 3$ simple cubic than the $d = 6$ simple cubic. Hence we have shown that dimension plays a more important role than coordination number or connectivity in determining the transition behaviour of the model nematogen, and that the results of the previous section may be interpreted as an effect of dimension.

3.3. *Finite-size effects*

We have made a partial study of finite-size effects by examining the $d = 6$ simple cubic system with linear dimensions $L = 3$, 4, and 5. Theoretically, for a first-order transition one expects the shift of the transition temperature from the thermodynamic limit to scale with the square root of the system volume [12] according to the relation

$$T_c^*(L = \infty) - T_c^*(L) \propto L^{-d/2}. \tag{7}$$

One also expects a smearing out of the transition associated with this shift, observed, for example, by a smoothing out of the discontinuity in the energy near

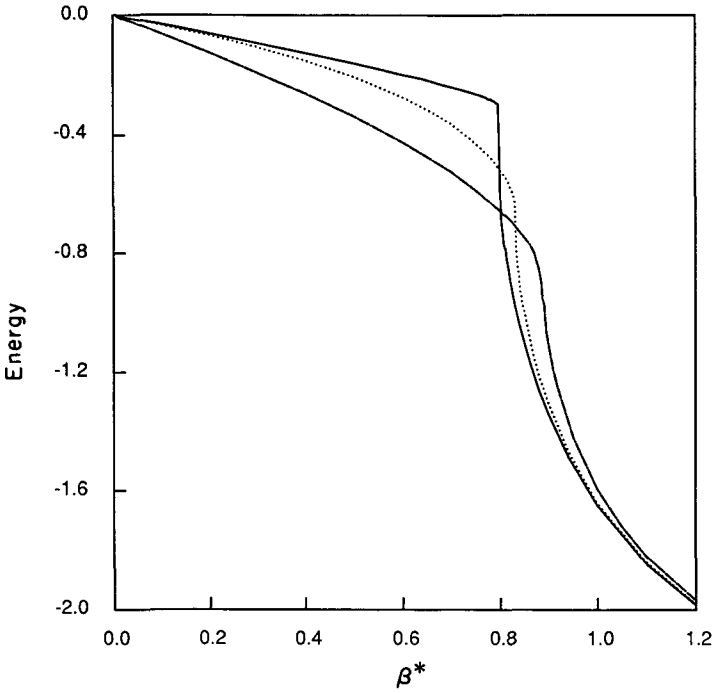

Figure 8. The internal energy U^* as a function of the inverse temperature β^* for simple cubic lattices of dimension $d = 6$ (full line) and $d = 3$ (dot–dashed), and for an f.c.c. lattice in $d = 3$ (dotted line).

the transition. Figure 9 illustrates this phenomenon for our case. The simulations performed do not provide the temperature resolution necessary for an accurate verification of equation (7). Rather, we assume that the equation holds, and use it along with our data to extrapolate the transition temperature to the thermodynamic limit corresponding to $L = \infty$. Table 4 shows the transition temperature obtained from the peak in the heat capacity of the heating runs, corresponding to the different linear dimensions, along with the approximate value of T_c^* ($L = \infty$) given by equation (7). We can see that our result for linear dimension $L = 4$ gives the correct transition temperature within the uncertainty of our value. In addition, from figure 9 one sees that $L = 4$ and $L = 5$ yield essentially the same discontinuity in the energy at the transition. We conclude that our system of size 4^6 is large enough to predict correct thermodynamic quantities. Since the scaling law only depends on the volume of the system and results for different dimensions were all obtained on

Table 4. Scaling in $d = 6$ simple cubic lattice.

L	β_c^*	T_c^*
3	0·802 ± 0·002	1·247 ± 0·003
4	0·800 ± 0·002	1·250 ± 0·003
5	0·799 ± 0·002	1·252 ± 0·003
∞	0·798	1·253

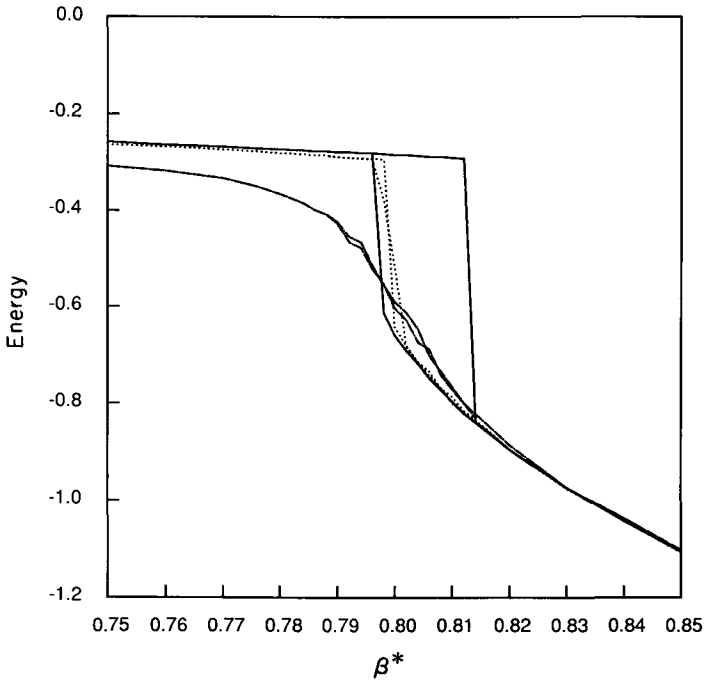

Figure 9. The internal energy U^* as a function of the inverse temperature β^* for 'heating' and 'cooling' runs of simple cubic systems in $d = 6$, with linear dimension $L = 5$ (solid line), $L = 4$ (dotted line) and $L = 3$ (dot–dashed line).

systems of approximately the same size, we can conclude also that the results for all dimensions are suitably converged to the thermodynamic limit.

As one can observe in figure 9, hysteresis is well pronounced for $L = 5$, but barely detectable for $L = 4$, and absent, within fluctuations, for $L = 3$. This is expected, since the system relaxation time increases much faster than linearly with the size of the system, and hence in large systems it is computationally difficult to equilibrate the system near the transition. One might ask how we determined the transition temperature for the $L = 6$ system whien the entire region is obscured by hysteresis. Clearly, when hysteresis is present one needs to know whether the heating or cooling run represents more accurately the equilibrium path of the system. One can also induce hysteresis by varying the rate at which the system is heated or cooled. By observing that the cooling curve collapses to the heating curve for a given system as the rate of heating and cooling is decreased, we determined that the heating run accurately predicts the location of the transition when hysteresis is present. This allowed us to determine the correct transition temperature for the 5^6 system even though hysteresis is present.

4. Concluding remarks

The transition properties of the spin model of the isotropic–nematic transition approach the mean-field results monotonically as the dimensionality is increased. From our data, there is an apparent power law scaling which describes the shift of the transition temperature with dimension from the mean-field result. If such a

'scaling law' exists for first-order transitions, it will have practical implications: given the mean-field result for the transition temperature, one could extrapolate back to the physical dimension of a given system to find the actual transition temperature. For this reason, we feel that investigation of this phenomenon for other first-order transitions is worthwhile.

From our studies, the isotropic–nematic transition is seen to be a very special consequence of three spatial dimensions, in which a tiny first-order transition—which is almost second-order—is observed. In two and four dimensions, the transition is *cleanly* second and first-order, respectively. A correct theoretical description of this 'small' first-order transition in $d = 3$ remains to be found.

This research was supported in part by the Petroleum Research Fund, administered by the American Chemical Society, and in part by Ford Research and NSF through the PYI program.

Appendix

Free energy calculation

The calculation of the low and high beta expansions of the free energy follows the derivation of Lebwohl and Lasher [3], generalized to arbitrary lattices and spatial dimensions. Here we summarize only the results of the calculations, noting where the results differ from the $d = 3$ simple cubic case considered by Lebwohl and Lasher, and give our results for the simple cubic lattice in d dimensions and for the f.c.c. lattice.

Low-$\beta\varepsilon$ expansion

We start from the N-particle partition function

$$Z_N = \int \left\{ \prod_{i=1}^{N} \frac{d\Omega_i}{4\pi} \right\} \exp\left[\beta\varepsilon \sum_{\langle i,j \rangle} P_2(\cos\theta_{ij}) \right], \tag{A 1}$$

where Ω_i are the angular coordinates of the ith spin, and the integration is over the orientations of the N spins. We then expand Z_N for small $\beta\varepsilon$ as a power series in $\beta\varepsilon$ to give

$$Z_N = \int \left\{ \prod_{i=1}^{N} \frac{d\Omega_i}{4\pi} \right\} \Bigg[1 + \beta\varepsilon \sum_{\langle i,j \rangle} P_2(\cos\theta_{ij}) + \tfrac{1}{2}(\beta\varepsilon)^2 \sum_{\langle i,j \rangle} \sum_{\langle k,l \rangle} P_2(\cos\theta_{ij}) P_2(\cos\theta_{kl}) + \tfrac{1}{6}(\beta\varepsilon)^3 \sum_{\langle i,j \rangle} \sum_{\langle k,l \rangle} \sum_{\langle m,n \rangle} P_2(\cos\theta_{ij}) P_2(\cos\theta_{kl}) P_2(\cos\theta_{mn}) + \ldots \Bigg], \tag{A 2}$$

where the sums run over all pairs of nearest neighbours. The first term of (A 2) is unity, and the second term is zero. Only the terms of the form $[P_2(\cos\theta_{ij})]^2$ contribute to the third term of (A 2). In addition, the fourth term contains terms of the form $[P_2(\cos\theta_{ij})]^3$ which do not occur for simple cubic lattices, but which do occur in general and result from the existence of closed triangles of nearest neighbour interactions.

Evaluating these integrals gives, for simple cubic lattices in d dimensions,

$$Z_N^{sc} = 1 + \frac{Nd}{10}(\beta\varepsilon)^2 + \frac{Nd}{105}(\beta\varepsilon)^3 + \ldots, \tag{A 3}$$

and for the f.c.c. lattice,

$$Z_N^{\text{fcc}} = 1 + \frac{3N}{5}(\beta\varepsilon)^2 + \left[\frac{2N}{35} + \frac{8N}{25}\right](\beta\varepsilon)^3 + \ldots, \tag{A 4}$$

where the second coefficient of $(\beta\varepsilon)^3$ is the contribution from the closed triangles of interactions. The free energy per particle $\beta f/d$ is

$$\beta\varepsilon\frac{f^{\text{sc}}}{d\varepsilon} = -\lim_{N\to\infty}\frac{\ln Z_N}{dN} = -\tfrac{1}{10}(\beta\varepsilon)^2 - \tfrac{1}{105}(\beta\varepsilon)^3 + \ldots, \tag{A 5}$$

$$\beta\varepsilon\frac{f^{\text{fcc}}}{6\varepsilon} = -\tfrac{1}{10}(\beta\varepsilon)^2 - \tfrac{11}{175}(\beta\varepsilon)^3 + \ldots \tag{A 6}$$

and the average energy per particle $\langle U\rangle/d$ is

$$\frac{\langle U\rangle^{\text{sc}}}{d\varepsilon} = \frac{\partial[\beta\varepsilon(f^{\text{sc}}/d\varepsilon)]}{\partial(\beta\varepsilon)} = -\tfrac{1}{5}(\beta\varepsilon) - \tfrac{1}{35}(\beta\varepsilon)^2 + \ldots \tag{A 7}$$

and

$$\frac{\langle U\rangle^{\text{fcc}}}{6\varepsilon} = -\tfrac{1}{5}(\beta\varepsilon) - \tfrac{33}{175}(\beta\varepsilon)^2 + \ldots. \tag{A 8}$$

Equations (A 7) and (A 8) compare well with the Monte Carlo energies for $\beta^* \leqslant 0{\cdot}4$.

High-$\beta\varepsilon$ expansion

Again starting from N-particle partition function (A 1), for $\beta\varepsilon$ sufficiently large, we assume that all spins are either parallel or antiparallel to the director. Following Lebwohl and Lasher [3], we expand the partition function to second order in the variables $\{x_i = \sin\theta_i\cos\phi_i,\ y_i = \sin\theta_i\sin\phi_i\}$, $i = 1, 2, \ldots, N$, where θ_i is the angle between the director and the orientation vector of the ith spin. Given the invariance of (A 1) under simultaneous rotation of all molecules of the lattice, and with spin 1 chosen to lie along the Z axis, the partition function becomes

$$Z_N = 4\pi(2^N)\int_{-\infty}^{\infty}\left\{\prod_{i=1}^{N}\frac{dx_i\,dy_i}{4\pi}\right\}\delta(x_1)\delta(y_1) \times \exp\left\{\beta\varepsilon\sum_{\langle i,j\rangle}1 - \tfrac{3}{2}[(x_i - x_j)^2 + (y_i - y_j)^2]\right\}, \tag{A 9}$$

where δ is the Dirac δ function and N is the number of spins in the system. The factor of 2^N comes from the degeneracy of the ground state since each spin can be either 'up' or 'down' with respect to the director. Rearranging the constant factors, we note that the integral is just the product of two identical integrals over the separate variables $\{x_i\}$ and $\{y_i\}$. Hence the partition function can now be written as

$$Z_N = \frac{2}{(2\pi)^{N-1}}I_N^2\exp\,[\beta\varepsilon Nz/2], \tag{A 10}$$

where z is the number of nearest neighbours per lattice site and

$$I_N = \int_{-\infty}^{\infty}dx^N\delta(x_0)\exp\left[-\tfrac{3}{2}\beta\varepsilon\sum_{\langle \mathbf{n},\mathbf{m}\rangle}(x_{\mathbf{n}} - x_{\mathbf{m}})^2\right]. \tag{A 11}$$

The index notation has been changed to show explicitly that the sums are over the lattice, and for convenience spin number 1 is chosen to be the spin at the origin 0. We change to 'spin-wave' variables, defined by

$$x_n = \frac{1}{\sqrt{N}} \sum_{\mathbf{k}} a_{\mathbf{k}} \exp(i\mathbf{k} \cdot \mathbf{n}) \tag{A 12}$$

Let $\{\tau\}$ be the set of real space vectors pointing to the nearest neighbours of a given lattice point. The sum over nearest neighbours in (A 11) becomes

$$\sum_{\langle \mathbf{n}, \mathbf{m} \rangle} (x_{\mathbf{n}} - x_{\mathbf{m}})^2 = \sum_{\mathbf{k}} |a_{\mathbf{k}}|^2 \sum_{\tau} (1 - \cos \mathbf{k} \cdot \tau) \tag{A 13}$$

The change of variables from $\{x_{\mathbf{n}}\}$ to $\{a_{\mathbf{k}}\}$ given by equation (A 12) is a unitary one, and hence the magnitude of the jacobian is unity. Since the integral in (A 11) is real, we ignore the phase factors and the $\{a_{\mathbf{k}}\}$ and choose limits of integration to yield a positive real result:

$$I_N = \int_{-\infty}^{\infty} da_{\mathbf{k}}\, \delta\left(\frac{1}{\sqrt{N}} \sum_{\mathbf{k}} a_{\mathbf{k}}\right) \exp\left[-\tfrac{3}{2}\beta\varepsilon \sum_{\mathbf{k}} a_{\mathbf{k}}^2 \sum_{\tau} (1 - \cos \mathbf{k} \cdot \tau)\right]. \tag{A 14}$$

When this integral is evaluated, the partition function becomes

$$Z_N = (6\beta\varepsilon) \exp(\beta\varepsilon N z/2)(3\beta\varepsilon)^{-N} N \prod_{\mathbf{k}}{}' \left(\sum_{\tau} 1 - \cos \mathbf{k} \cdot \tau\right)^{-1}. \tag{A 15}$$

In the limit $N \to \infty$ the free energy is

$$\beta f = -\tfrac{1}{2}\beta\varepsilon z + \ln(3\beta\varepsilon) + \frac{V_c}{(2\pi)^d} \int d\mathbf{k} \ln\left(z - \sum_{\tau} \cos \mathbf{k} \cdot \tau\right), \tag{A 16}$$

where V_c is the volume of the real space unit cell and the integral is taken over a unit cell in reciprocal space. For the cases of a d dimensional simple cubic lattice and the f.c.c. lattice, the free energies per particle are

$$\frac{1}{d}\beta f = -\beta\varepsilon + \frac{1}{d} \ln \beta\varepsilon + K(d), \qquad \text{(simple cubic)} \tag{A 17}$$

and

$$\tfrac{1}{6}\beta f = -\beta\varepsilon + \tfrac{1}{6} \ln \beta\varepsilon + K(\text{f.c.c.}), \qquad \text{(f.c.c. lattice)} \tag{A 18}$$

where the constant term K depends only on the lattice type and dimensionality. The integrals have been evaluated numerically, taking special care with the logarithmic divergence in the integrand of (A 16), and the values of the constant K for simple cubic lattices with $d = 2, \ldots, 7$ and the f.c.c. lattice are given in table A 1. For the

Table A 1. Free energy constant K.

d	Constant K
2	1·13243
3	0·92400
4	0·77458
5	0·66822
6	0·58921
7	0·52818
f.c.c.	0·58391

internal energy we obtain

$$\frac{2\langle U\rangle}{z\varepsilon} = -1 + \frac{2}{z\beta\varepsilon} \tag{A 19}$$

This expression is valid for any lattice.

References

[1] FRENKEL, D., LEKKERKERKER, H. N. W., and STROOBANTS, A., 1988, *Nature, Lond.*, **332**, 822.

[2] STROOBANTS, A., LEKKERKERKER, H. N. W., and FRENKEL, D., 1987, *Phys. Rev. Lett.*, **57**, 1452.

[3] LEBWOHL, P. A., and LASHER, G., 1972, *Phys. Rev.* A, **6**, 426; 1973, *Ibid.*, **7**, 2222.

[4] FISHER, M. E., 1974, *Rev. mod. Phys.*, **46**, 597.

[5] MAIER, W., and SAUPE, A., 1958, *Z. Naturf.* (*a*), **13**, 564; 1959, *Ibid.*, **14**, 882; 1960, *Ibid.*, **15**, 287.

[6] FABBRI, U., and ZANNONI, C., 1986, *Molec. Phys.*, **58**, 763.

[7] REMLER, D. K., and HAYMET, A. D. J., 1986, *J. phys. Chem.*, **90**, 5426.

[8] BINDER, K., 1986, *Z. Phys.* B, 61, 13.

[9] METROPOLIS, N., ROSENBLUTH, A. W., ROSENBLUTH, M. N., TELLER, A. H., and TELLER, E., 1953, *J. chem. Phys.*, **21**, 1087.

[10] LUCKHURST, G. R., and SIMPSON, P., 1982, *Molec. Phys.*, **47**, 251.

[11] VAN DER HAEGEN, R., DEBRUYNE, J., LUYCKX, R., and LEKKERKERKER, H. N. W., 1980, *J. chem. Phys.*, **73**, 2469.

[12] BINDER, K., 1986, *Monte Carlo Methods in Statistical Physics*, edited by K. Binder (Springer-Verlag), Chap. 10.